Direct Determination of Metastable Phase Diagram by Synchrotron Radiation Experiments on Undercooled Metallic Melts

C. Notthoff,[1] B. Feuerbacher,[1] H. Franz,[2] D. M. Herlach,[1] and D. Holland-Moritz [1,3]

[1]*Institut für Raumsimulation, DLR, D-51170 Köln, Germany*
[2]*HASYLAB at DESY, Notkestraße 85, D-22603 Hamburg, Germany*
[3]*Institut für Experimentalphysik IV, Ruhr-Universität Bochum, D-44780 Bochum, Germany*
(Received 1 March 2000)

The phase selection process during the crystallization of undercooled metallic melts is studied *in situ* by combining the electromagnetic levitation technique with energy dispersive x-ray diffraction of synchrotron radiation. The crystallization of metastable bcc phase in binary Ni-V alloys was identified. A metastable phase diagram of Ni-V alloy is constructed, which shows the primarily solidifying phase as a function of composition and undercooling. The analysis within nucleation theory emphasizes the important role of metal oxide as a heterogeneous nucleation site controlling the phase selection.

If a melt is undercooled below its equilibrium melting temperature the liquid becomes metastable. The excess free energy of the undercooled melt can be used by the system to form metastable solids [1]. The variety of such metastables ranges from supersaturated and grain-refined alloys, metastable crystallographic structures, disordered superlattice structures of intermetallics, and even amorphous metals [2].

A metastable solid shows a smaller melting temperature than the stable solid phase [3]. Hence, an undercooling exceeding the difference between equilibrium melting temperature and melting temperature of the respective metastable solid is needed to generate a driving force for its solidification. Electromagnetic levitation was extensively used for containerless undercooling and solidification of metals and alloys [2]. A freely suspended drop offers the benefit of a large undercooling range and that the undercooled melt is accessible for direct observation of rapid solidification [4].

Temperature-time profiles measured during undercooling and solidification of electromagnetically processed samples show an increase in temperature during crystallization (recalescence) up to the melting temperature of the solidifying phase owing to the rapid release of the heat of crystallization. Undercooling experiments on binary Fe-Ni alloys reveal two-step recalescence profiles which were interpreted by a primary solidification of a metastable bcc phase (at Ni concentrations larger than 4 at. %) during the first step followed up by the crystallization of the remaining melt to stable fcc phase during the second step [5]. The temperature after recalescence, called postrecalescence temperature, of the variously concentrated alloys correspond to the liquidus temperatures of stable fcc and metastable bcc phases, respectively. However, the metastable bcc phase could not be detected in the as-solidified sample at ambient temperatures. Primarily formed bcc was either remelted during the second step of recalescence, i.e., during solidification of stable fcc phase, or it was transformed by a solid state reaction during

cooling the as-solidified sample to ambient temperatures at small cooling rates (a few K/s). Similar observations were reported for Fe-Ni-Cr [6] and Ni-V [7] alloys.

The conclusions of the aforementioned undercooling experiments are based upon the analysis of the thermodynamics. They do not directly evidence the primary solidification of metastable bcc phase in the undercooled melt. The "lifetime" τ of the metastable phase is too short to record a diffraction pattern by conventional diffraction and to identify the crystallographic phase unambiguously. The situation is changed if high intensity synchrotron radiation is considered. It was shown that diffraction experiments using synchrotron radiation on metallic glasses are able to directly observe and to identify the crystalline phases which are formed during devitrification of the glassy state [8,9]. Recently, conical nozzle levitation was combined with diffraction of synchrotron radiation to study the short-range order in undercooled boron liquids [10]. Electromagnetic levitation for containerless undercooling and solidification of metals was applied to provide direct interaction of the sample with probes, such as muons [11], positrons [12], and photons [13].

In the present work the electromagnetic levitation technique to undercool bulk samples was combined with energy dispersive x-ray diffraction (EDXD) to record *in situ* complete diffraction patterns during crystallization of stable and metastable phases in undercooled metallic melts.

The EDXD experiments were performed at the white beam Laue beam line ID 09 at the European Synchrotron Radiation Facility in Grenoble, France. Unfocused radiation from a wiggler with an energy range from 7 to 148 keV and an energy dispersive germanium detector at a constant scattering angle of 5° was used. The experimental setup is described in detail elsewhere [14]. The minimum integration time to observe a spectrum of reasonable quality was 0.5 s, which is the limiting factor for observing time resolved phase selection in undercooled samples.

While the lifetime τ of metastable bcc structures in Fe-Ni and Fe-Ni-Cr alloys is within ms [5,6], considerably longer times were reported for some Ni-V alloys ranging from several ms for Ni-rich alloys and some s for V-rich alloys [7]. Considering the time resolution of the detector, we have investigated the binary Ni-V system in the composition range between 42 and 63 at. % V. In this composition range Ni-V shows a phase competition of three different crystallographic phases, bcc, fcc, and the intermetallic σ' phase. The σ' phase shows a complex tetragonal structure within 30 atoms per unit cell.

The samples of about 0.9 g in mass and 5–6 mm in diameter were alloyed from the elements Ni and V (both of purity better than 99.9%) in an arc furnace under Ar atmosphere. The alloys were undercooled and solidified within the electromagnetic levitation chamber, especially designed for this kind of experiment [14]. The temperature T was controlled by forced convection cooling of H_2-He gas and measured by a two color pyrometer in top view with an absolute accuracy of ± 10 K and a relative accuracy of ± 1 K. Complete cycles of melting, heating, undercooling, and solidification were recorded. The nucleation temperature T_N was inferred from the respective temperature-time profiles by the onset of recalescence and the undercooling ΔT was determined from the difference of liquidus temperature, T_L, and the nucleation temperature, T_N, thus $\Delta T = T_L - T_N$.

As an example, Fig. 1 shows a temperature-time profile (cf. inset) and four diffraction spectra recorded during undercooling and solidification of a levitated $Ni_{41}V_{59}$ sample. In the temperature-time profile a double recalescence is observed. The first recalescence peak sets in at an undercooling of $\Delta T = 50$ K ($T_N = 1493$ K) and T rises up to $T = 1514$ K being below the liquidus temperature of the stable σ' phase, $T_L^{\sigma'} = 1543$ K. After 57 s, the remaining undercooled liquid crystallizes in a subsequent step and T rises up to 1490 K. This temperature is below the liquidus temperatures of both the metastable bcc phase, $T_L^{bcc} = 1533$ K, and the stable σ' phase, $T_L^{\sigma'}$. Hence, the determination of the postrecalescence temperatures does not allow for the discrimination of the phases solidified during the two different recalescence events. The crystalline structures of the solidifying phases were directly identified by the diffraction pattern immediately recorded after the two recalescence events as shown in Fig. 1. The first spectrum has been taken on the undercooled liquid at $T = 1495$ K (1), the second one (2) directly after the first recalescence event, and the third one (3) 54 s after that event. Spectrum 2 clearly reveals that after the first recalescence event (denoted by I in Fig. 1) a part of the undercooled melt crystallized into metastable bcc phase which grows continuously upon further cooling as shown by spectrum 3. In both spectra the Bragg peaks are identified as the (110), (200), and (211) reflections of the metastable bcc phase. In a second reaction the remaining liquid crystallizes into the stable σ' phase as indicated by spectrum 4 of Fig. 1. The Bragg interferences of the
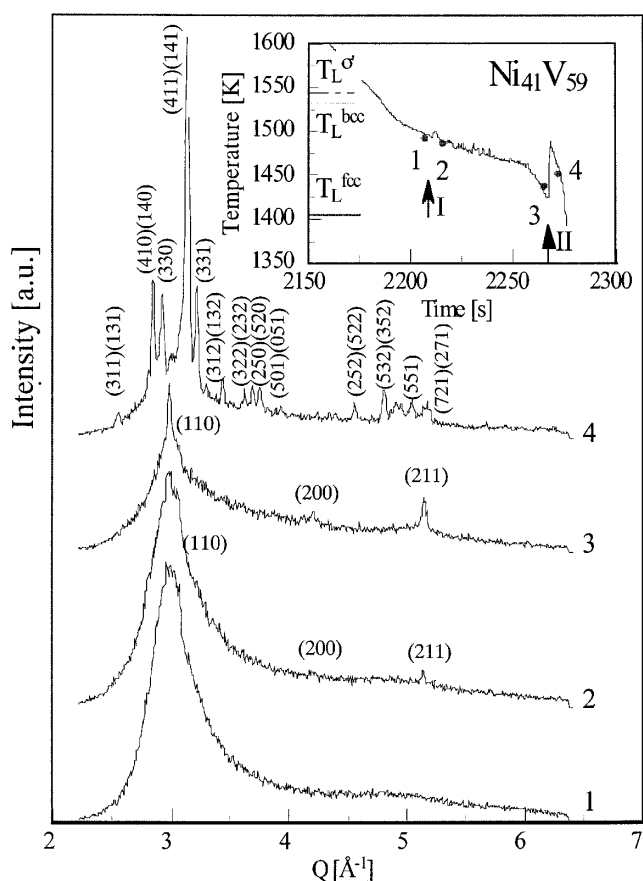

FIG. 1. Energy dispersive x-ray diffraction spectra recorded during undercooling and solidification of a levitated $Ni_{41}V_{59}$ at a constant diffraction angle of $2\Theta = 5°$. A part of the undercooled melt (spectrum 1) primarily crystallizes into the metastable bcc phase (spectra 2 and 3) followed up by the crystallization of the intermetallic σ' phase (spectrum 4). The bcc phase disappears by transforming during the second solidification period. The inset marks the temperature and time during cooling at which the various spectra are recorded. The arrows denoted by I and II mark the two recalescence events of primary bcc crystallization and secondary σ' crystallization.

bcc phase disappear during the second solidification process, indicating that the metastable bcc phase transforms during the temperature rise at the second recalescence event.

The analysis of equivalent x-ray diffraction experiments performed on samples of different composition and solidified at various levels of undercooling leads to the development of a phase selection diagram of Ni-V shown in Fig. 2. The equilibrium liquidus (T_L) and solidus temperatures (T_S) of fcc, bcc, and σ' phases [15] are exhibited by solid lines, and the extensions of T_L for all phases into the metastable region of the undercooled melt are represented by dashed (bcc), dotted (fcc), and dash-dotted (σ') lines. The equilibrium phase diagram and the metastable extensions of the T_L of the respective phases are calculated according to the model by Kaufman [16]. The symbols denote the *primarily* solidified phase as a function of composition and nucleation temperature: fcc phase (open
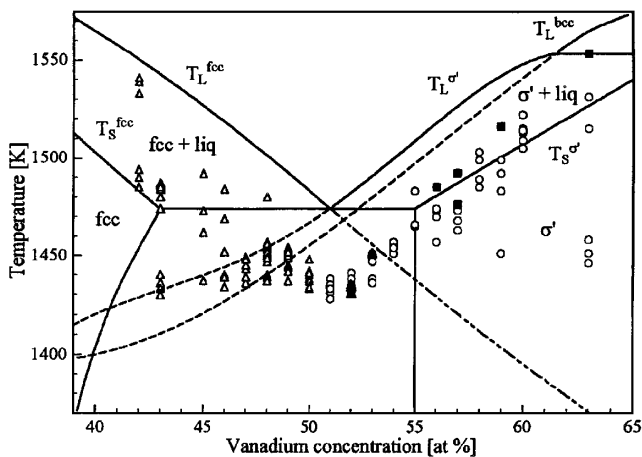
FIG. 2. Phase selection diagram of Ni-V. The different symbols mark the primarily solidified phases as a function of composition and nucleation temperature: open triangles: fcc phase; closed triangles: fcc phase $+ \sigma'$ phase; open circles: bcc phase; and closed squares: σ' phase. The solid lines give the equilibrium liquidus and solidus temperatures while dash, dotted, and dash-dotted lines represent the metastable extensions of liquidus temperatures of bcc, σ', and fcc phase, respectively.

triangles), bcc phase (open circles), fcc phase $+ \sigma'$ phase (closed triangles), and σ' phase (closed squares).

The comparison of the experimental results with the calculated phase diagram shows that the formation of the metastable bcc phase is observed in the concentration range between 51 and 60 at.% V at nucleation temperatures below the metastable extension of bcc liquidus, i.e., in a temperature and concentration regime in which a driving force for the solidification of bcc phase does exist: $\Delta G_V = G(\text{bcc}) - G(L) < 0$ [$G(\text{bcc})$ and $G(L)$: Gibbs free energy of bcc solid and liquid]. This is a necessary but not a sufficient condition for the formation of metastable bcc phase. Usually, ΔG_V is largest for the stable phase in comparison with any metastable solid [3]. Crystallization of metastable solids can be understood, if nucleation processes are taken into account.

According to the classical nucleation theory the formation of a nucleus of critical size requires an activation energy ΔG^* [17]:

$$\Delta G^* = \frac{16\pi}{3} \frac{\sigma^3}{\Delta G_V^2} f(\Theta), \tag{1}$$

where σ is the energy of the solid-liquid interface and $f(\Theta)$ the catalytic potency factor for heterogeneous nucleation. σ is estimated within the negentropic model [18,19]

$$\sigma = \alpha \frac{\Delta S_f}{N_A^{1/3} V_m^{2/3}} T, \tag{2}$$

where ΔS_f is the entropy of fusion, N_A Avogadro's number, and V_m the molar volume. The factor α depends on the structure of the solid nucleus, $\alpha(\text{fcc}) = 0.86$ and $\alpha(\text{bcc}) = 0.71$ [19] while $\alpha(\sigma'$ phase$) = 0.36$ [20]. Assuming equal $f(\Theta)$'s for all phases Eq. (2) predicts the interfacial energy being smallest for the σ' phase, medium for the bcc phase, and largest for the fcc phase. Thus,

the primary crystallization of the metastable bcc phase in competition with the fcc phase in the $\text{Ni}_{41}\text{V}_{59}$ alloy can be understood by a smaller ΔG^* for the metastable bcc phase because of its smaller σ according to Eqs. (1) and (2). But the interfacial energy of the σ' phase is even less than that of the bcc phase, $\sigma(\sigma') < \sigma(\text{bcc})$, suggesting an energetic preference of nucleation of σ' phase, $\Delta G^*(\sigma') < \Delta G^*(\text{bcc})$, apparently in contrast to the experiment, $\Delta G^*(\sigma') > \Delta G^*(\text{bcc})$.

According to Eq. (1) the lower activation energy $\Delta G^*(\text{bcc}) < \Delta G^*(\sigma')$ can be understood within nucleation theory by a corresponding difference of the catalytic potencies $f(\Theta)$ being smaller for the bcc phase than for the σ' phase. In case of Ni-V alloys one has to consider Ni and V oxides as potential heterogeneous nucleation sites. NiO and VO show crystallographic structures of NaCl type [21] and are solid in the investigated temperature range [22]. VO and V_2O_3 are more stable compared with NiO [23] and cannot be reduced by annealing in H_2 atmosphere at temperatures $T < 2000$ K. Thus, solid vanadium oxides will be present at the surface of the molten alloy during levitation processing. In fact, the existence of thin oxide layers on the surface of the as-processed samples was proved by field-ion spectroscopy [24]. Metal oxides possess in general a higher emissivity than pure metals. This leads to a contrast of brightness in video observation. From video images it is estimated that the oxides cover less than 10% of the surface area of Ni-V alloys.

For further discussion $f(\Theta)$ is determined from the results of the undercooling experiments. It is assumed that at least one nucleation event is sufficient to initiate the solidification of the undercooled melt of volume V during the experiment time t_N. This means

$$I_{ss}(T_N) \cdot V \cdot t_N \geq 1 \tag{3}$$

with I_{ss} the steady state nucleation rate, V the volume of the sample, and $t_N = \Delta T/(dT/dt)$ the experiment time. t_N is calculated by the undercooling ΔT and the cooling rate dT/dt, both of which are taken from the measured temperature-time profiles. The steady state nucleation rate I_{ss} is given by [17]

$$I_{ss} = \frac{k_B T \xi N_A}{3\eta(T)a_0^3} \exp\left(-\frac{16\pi\sigma^3}{3\Delta G_V^2 k_B T} f(\Theta)\right) \tag{4}$$

with η the viscosity calculated according to a Vogel-Fulcher expression

$$\eta = \eta_0 \exp\left(\frac{A}{T - T_0}\right). \tag{5}$$

a_0 is the interatomic spacing and is computed from the ratio V_m/N_A, k_B Boltzmann's constant, T_0 the ideal glass transition temperature (assumed to be $T_0 = T_L/3$), A and η_0 numerical parameters for the calculation of the viscosity, and ξ the fraction of atoms acting as nucleation sites assuming that 10% of the surface atoms are in contact with metal oxide. For the calculation of I_{ss} the numerical values are used as given in Table I. ΔG_V is approximated by the model of Kaufman and σ is calculated using

TABLE I.   Characteristic parameters of $Ni_{41}V_{59}$ alloy as used for the calculation of the steady state nucleation rate I_{ss}.

Parameter	bcc phase	σ' phase
T_L [K]	1533	1543
ΔG_V (T_N) [J]	-996	-1494
ΔS_f [J K/mole]	12.31	16.42
V_m [cm^3/mole]	7.7	7.7
α	0.71	0.36
V [cm^3]	0.11	0.11
t_N [s]	31	31
ξ	10^{-10}	10^{-10}
η_0 [poise]	0.1	0.1
A [K]	2000	2000

Eq. (2). $f(\Theta)$ is determined as free parameters for the nucleation of bcc and σ' phases, such that Eq. (3) describes the undercooling experiment at which nucleation of the respective phase is observed at the maximum undercooling (here $\Delta T = 91$ K). This gives $f(\Theta) = 0.0143$ for the metastable bcc phase and $f(\Theta) = 0.0997$ as a lower limit for the stable σ' phase for the $Ni_{41}V_{59}$ alloy. Obviously, the heterogeneous nucleation site shows different $f(\Theta)$'s for the crystallization of bcc and σ' phases. $f(\Theta)$ should be higher the more similar the crystallographic structures of heterogeneous nucleation sites and the solidifying phase [17]. The σ' phase is a Frank-Kasper phase with a complex polytetrahedral structure [25]. The NaCl type structure of the VO shows more similarity to the cubic structure of bcc and fcc phases than to the polytetrahedral structure of the σ' phase. Consequently, $f(\Theta)$ for heterogeneous nucleation on Ni and V oxides is expected to be larger for the σ' phase than for the cubic bcc phase; hence $\Delta G^*(\text{bcc}) < \Delta G^*(\sigma')$, in qualitative agreement with the experimental findings.

In summary, the electromagnetic levitation technique for containerless undercooling of bulk melts was combined with energy dispersive x-ray diffraction to directly observe the phase selection process during solidification of undercooled Ni-V melts. The analysis of all data leads to the construction of a phase selection diagram for Ni-V which describes the formation of different phases, stable or metastable, as a function of alloy composition and undercooling. The results are discussed in the framework of heterogeneous nucleation revealing the importance of solid metal oxides on the heterogeneous nucleation and the preselection of crystalline phases during solidification of undercooled metallic melts.

[1] B. Feuerbacher, Mater. Sci. Eng. **R4**, 1 (1989).
[2] D. M. Herlach, Mater. Sci. Eng. **R12**, 177 (1994).
[3] D. Turnbull, in *Undercooled Alloy Phases,* edited by E. W. Collings and C. C. Koch, Proceedings of the Hume-Rothery Memorial Symposium, New Orleans, 1986 (Metallurgical Society, Warrendale, PA, 1987), p. 3.
[4] R. Willnecker, D. M. Herlach, and B. Feuerbacher, Phys. Rev. Lett. **62**, 2707 (1989).
[5] E. Schleip, D. M. Herlach, and B. Feuerbacher, Europhys. Lett. **11**, 751 (1990).
[6] T. Volkmann, W. Löser, and D. M. Herlach, Metall. Mater. Trans. A **28**, 461 (1997).
[7] J. Schroers, T. Volkmann, D. M. Herlach, D. R. Allen, and J. H. Perepezko, Int. J. Rapid Solidif. **9**, 267 (1996).
[8] M. Sutton, Phys. Rev. Lett. **62**, 288 (1989).
[9] S. Brauer, J. O. Ström-Olsen, M. Sutton, Y. S. Yang, A. Zaluska, G. B. Stephenson, and U. Köster, Phys. Rev. B **45**, 7704 (1992).
[10] S. Krishnan, S. Ansell, J. J. Felten, K. J. Volin, and D. L. Price, Phys. Rev. Lett. **81**, 576 (1998).
[11] D. Herlach, C. Bührer, D. M. Herlach, K. Maier, C. Notthoff, D. Platzek, and J. Reske, Europhys. Lett. **44**, 98 (1998).
[12] C. Bührer, U. Holzwarth, K. Maier, D. Platzek, and J. Reske, Z. Phys. A **63**, 191 (1996).
[13] G. Jacobs and I. Egry, Phys. Rev. B **59**, 3961 (1999).
[14] C. Notthoff, H. Franz, M. Hanfland, D. M. Herlach, D. Holland-Moritz, and W. Petry, Rev. Sci. Instrum. **71**, 3791 (2000).
[15] T. B. Massalski, *Binary Alloy Phase Diagrams* (The Materials Information Society, Materials Park, OH, 1996), 3rd printing.
[16] L. Kaufman, in *Proceedings of the International Conference on Alloy Phase Diagrams* (American Society of Metals, Metals Park, OH, 1986), p. 59.
[17] J. W. Christian, in *The Theory of Transformation in Metals and Alloys* (Pergamon Press, New York, 1975).
[18] F. Spaepen and R. B. Meyer, Scr. Metall. **10**, 257 (1976).
[19] C. V. Thompson, Ph.D. thesis, Harvard University, 1979.
[20] D. Holland-Moritz, Int. J. Non-Equilib. Process. **11**, 169 (1998); Mater. Sci. Eng. A (to be published).
[21] *Kristallstrukturdaten anorganischer Verbindungen,* Landolt-Börnstein, Bd. 7 b (Springer-Verlag, Berlin, Heidelberg, New York, 1975).
[22] I. Barin, *Thermochemical Data of Pure Substances* (VCH, Weinheim, 1995), Vol. 2, 3rd ed.
[23] H. Schmalzriedt and A. Navrotzky, *Festkörperthermodynamik: Chemie des festen Zustands* (Verlag Chemie, Weinheim, 1975).
[24] The authors express their thanks to M. Weiner and A. Wieck, Ruhr-University Bochum, for the surface investigations of the samples by field-ion spectroscopy.
[25] F. C. Frank and J. S. Kasper, Acta Crystallogr. **11**, 184 (1958).